Biochemical and Biophysical Research Communications 437 (2013) 642–647

Contents lists available at SciVerse ScienceDirect

Biochemical and Biophysical Research Communications

journal homepage: www.elsevier.com/locate/ybbrc

The Kunitz-protease inhibitor domain in amyloid precursor protein reduces cellular mitochondrial enzymes expression and function

Li-Min Chua, Mei-Li Lim, Boon-Seng Wong *

Department of Physiology, Yong Loo Lin School of Medicine, National University of Singapore, Singapore

ARTICLE INFO

Article history:
Received 2 July 2013
Available online 16 July 2013

Keywords:
Metabolic enzymes
KPI
APP
Mitochondrial function

ABSTRACT

Mitochondrial dysfunction is a prominent feature of Alzheimer's disease (AD) and this can be contributed by aberrant metabolic enzyme function. But, the mechanism causing this enzymatic impairment is unclear. Amyloid precursor protein (APP) is known to be alternatively spliced to produce three major isoforms in the brain (APP695, APP751, APP770). Both APP770 and APP751 contain the Kunitz Protease Inhibitory (KPI) domain, but the former also contain an extra OX-2 domain. APP695 on the other hand, lacks both domains. In AD, up-regulation of the KPI-containing APP isoforms has been reported. But the functional contribution of this elevation is unclear. In the present study, we have expressed and compared the effect of the non-KPI containing APP695 and the KPI-containing APP751 on mitochondrial function. We found that the KPI-containing APP751 significantly decreased the expression of three major mitochondrial metabolic enzymes; citrate synthase, succinate dehydrogenase and cytochrome c oxidase (COX IV). This reduction lowers the NAD^+/NADH ratio, COX IV activity and mitochondrial membrane potential. Overall, this study demonstrated that up-regulation of the KPI-containing APP isoforms is likely to contribute to the impairment of metabolic enzymes and mitochondrial function in AD.

1. Introduction

A key neuropathological feature of Alzheimer's disease (AD) is the presence of extracellular amyloid plaques composed of the amyloid β-peptide, which is derived from the transmembrane amyloid precursor protein (APP) [1,2]. APP is encoded by a single 19-exon gene on chromosome 21 [3]. Exons 7, 8 and 15 of the APP gene can be alternatively spliced to produce multiple isoforms. In the brain, there are three major APP isoforms (APP695, APP751, APP770) [4], and APP695 is the predominant splice variant. These transcripts code for protein species containing 695, 751 and 770 amino acids, respectively. Exons 7 and 8 specifically encode a 56-amino acid Kunitz-type Proteinase Inhibitor (KPI) domain and a 19-amino acid domain that shares sequence identity with the OX-2 antigen of thymus-derived lymphoid cells. Both APP770 and APP751 contain the KPI domain, but the former also contain an extra OX-2 domain. APP695 on the other hand, lacks both domains.

Studies have reported that the KPI-containing APP isoforms (APP751/770) are up-regulated in AD brain [5–8]. Several functions have been suggested for the KPI domain on APP [9–11], including the inhibition of serine proteases. Further, cells expressing APP with and without the KPI domain (APP695, APP751) was found to have different susceptibility toward α-and β-secretase cleavage, affecting Aβ production [12,13].

Mitochondrial dysfunction is a prominent feature in Alzheimer's disease (AD) [14,15] and this deficit is likely contributed by defective expression and function of metabolic enzymes, leading to increased production of free radicals [16–21]. However, the cause(s) leading to the down-regulation of these metabolic enzymes is unclear. Furthermore, the functional connection between the increasing generation of the KPI-containing APP isoforms and the detected mitochondrial dysfunction is unknown.

In this study, we have expressed APP695 and APP751 in the APP-null neuronal cell line [22], to compare the effect of these two APP isoforms on mitochondrial function. We found that the KPI-containing APP751 lead to lower expression of major mitochondrial metabolic enzymes. This reduction leads to lower mitochondrial membrane potential, cytochrome c oxidase activity and NAD/NADH ratio in cells expressing APP751.

2. Materials and methods

2.1. Plasmids, cell culture and transfection

The cDNAs for human APP695 (KPI-APP) and APP751 (KPI + APP) bearing the C-terminal Swedish mutations [23] were kindly provided by Dr. Man-Sun Sy (Case Western Reserve

* Corresponding author.
E-mail address: bswong@nus.edu.sg (B.-S. Wong).

0006-291X/$ - see front matter © 2013 Elsevier Inc. All rights reserved.
http://dx.doi.org/10.1016/j.bbrc.2013.07.022

University, USA) and cloned into the expression vector pcDNA6.2-DEST (Life Technologies).

The APP-knockout (APP-KO) cell line [22] was grown in DMEM supplemented with 10% fetal bovine serum, 5% penicillin–streptomycin-amphotericin B and 5% sodium pyruvate, and maintained at 37 °C in a humidified incubator supplied with 5% CO_2. Expression vectors containing no insert (mock), APP695 and APP751 were stably transfected into the APP-KO cells using Fugene 6 reagent (Roche) according to manufacturer's instructions. Selection for cells containing the required construct was performed in DMEM with 5 μg/ml blasticidin (Life Technologies). Selected clones were maintained in DMEM containing 2.5 μg/ml blasticidin (Life Technologies).

2.2. SDS–PAGE and Western blot analysis

Cells were lysed in ice-cold 1× RIPA buffer (Cell Signaling Technology) containing protease inhibitors cocktail tablet (Roche) before subjecting to brief sonication and centrifugation. Cellular samples (30 or 40 μg of protein) were resolved on 7–15% tris–glycine sodium dodecyl sulfate–polyacrylamide gel electrophoresis (SDS–PAGE) and transferred to nitrocellulose membrane (Biorad). The membranes were probe with the respective primary antibodies before incubation with horseradish peroxidase (HRP)-conjugated secondary antibodies. The reactive protein bands were visualized by chemiluminescence using the SuperSignal® West Dura Substrate (Pierce) system. Pre-stained Precision Plus protein standards (Biorad) were used to calculate the apparent molecular weight of the protein bands.

Immunoblotting of APP was performed using two anti-APP antibodies. Monoclonal antibody 22C11 (Millipore) recognize the N-terminal of human APP (REFS) and 6E10 (Covance) recognizes the C-terminal of human APP (REFS).

Immunoblotting of β-actin using a rabbit polyclonal antibody that binds to the C-terminal of β-actin (Sigma) was included in all Western blot analysis to ensure comparable protein loading. Each immunoblotting was repeated up to three times using different preparations of the same cell line.

2.3. Real-time quantitative PCR

Total RNA was isolated from the cells using TRIzol® reagent (Life Technologies) before conversion to cDNA using the AMV reverse transcriptase (Promega). Expression level of the following human and mouse genes (and the TaqMan Gene Expression Assay catalogue) was investigated using real-time quantitative PCR and TaqMan probe-based chemistry (Applied Biosystems); human APP695 (Hs01562345_m1), human APP751 (Hs01562342_m1), human APP (Hs01552283_m1), mouse citrate synthase (Mm00466043_m1), mouse succinate dehydrogenase (Mm00458268_m1), mouse cytochrome C oxidase (Mm01250094_m1) and mouse β-actin (Mm00607939_s1). These probes span the exon(s) of the targeted

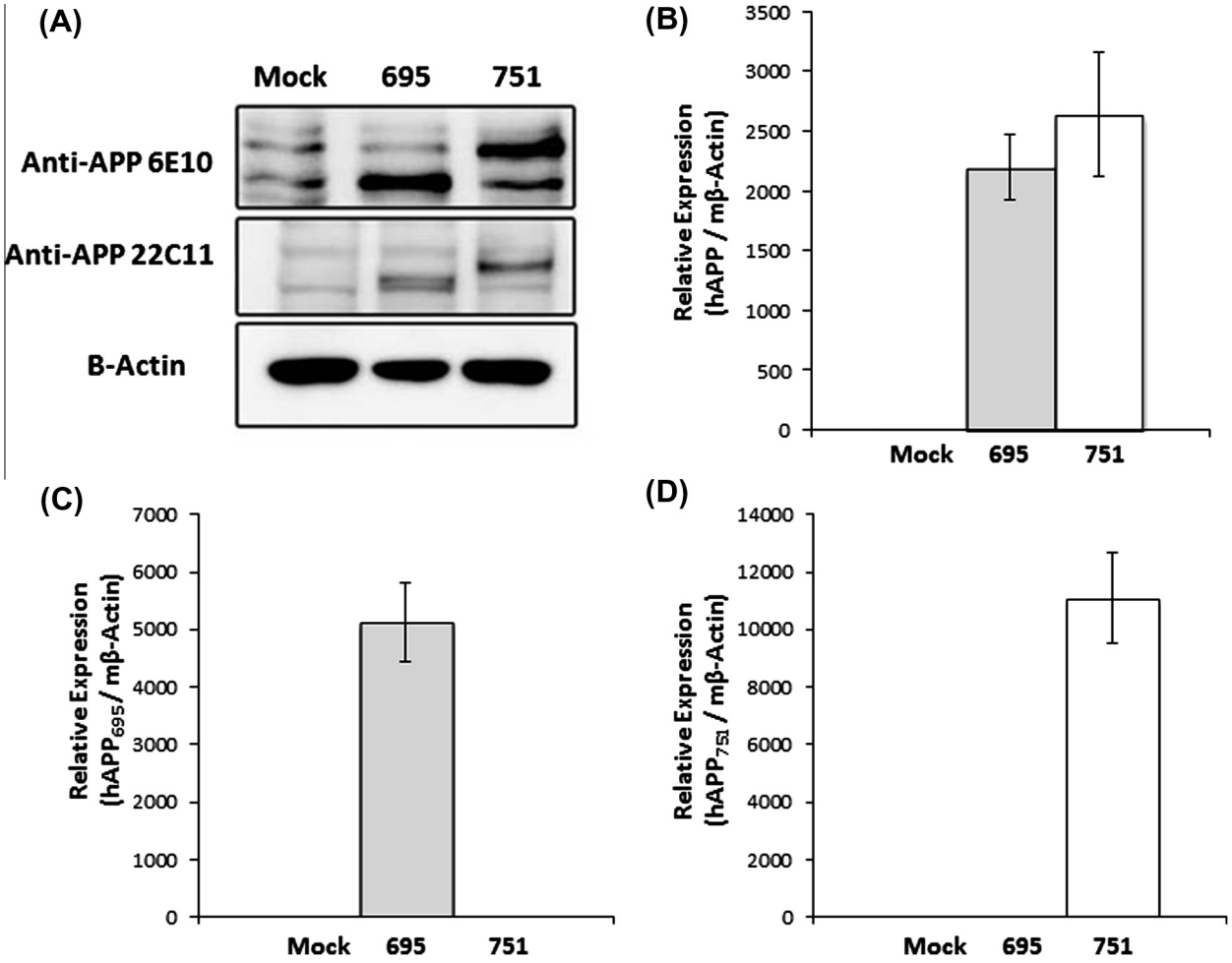

Fig. 1. APP isoforms expression. (A) Immunoblotting of APP in the mock-transfected cell line and transfected cells expressing APP695 and APP751. APP was immune-detected using anti-APP 6E10 and anti-APP 22C11. β-actin was immunoblotted to ensure similar gel loading of the starting material in each sample. Real-time PCR quantification of (B) total APP, (C) APP695 and (D) APP751 expression in the stably-transfected mock, APP695 and APP751 expressing cell lines. The expression of the targeted gene was quantified relative to the endogenous β-actin level for each sample. Each value represents the mean ± SEM of three assays for each cell line sample.

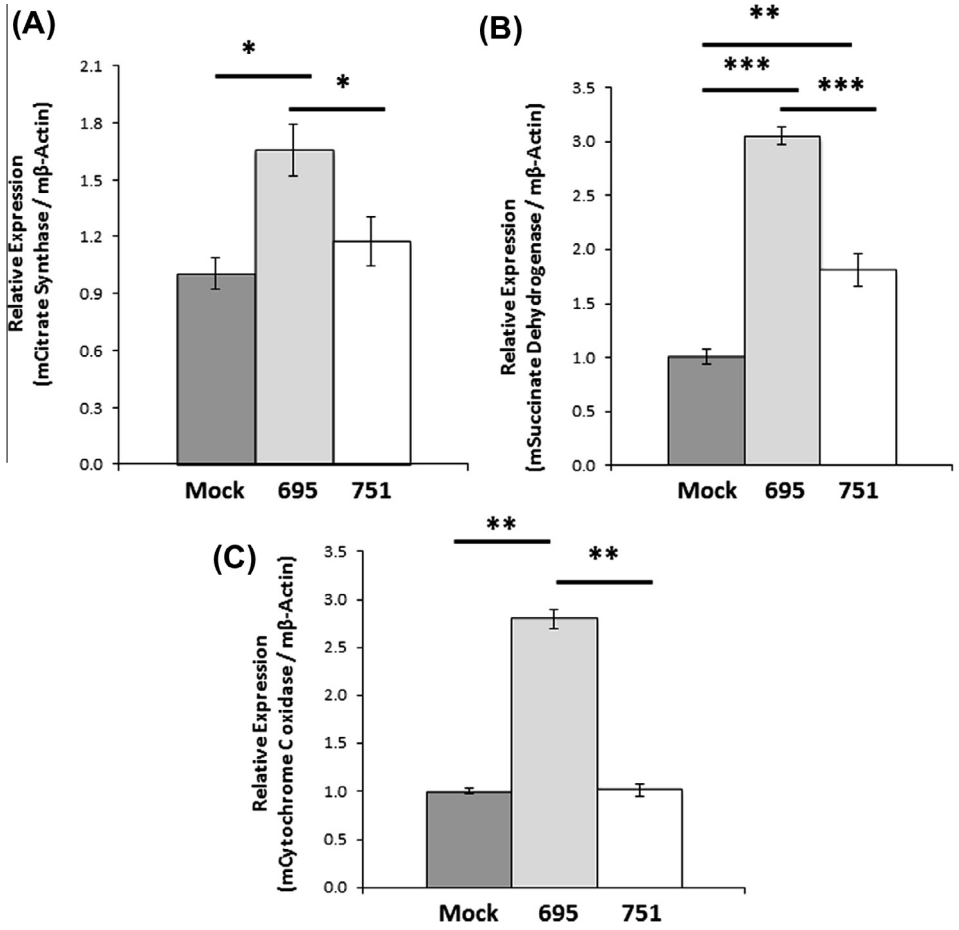

Fig. 2. Cells expressing APP751 reduce mitochondrial metabolic enzymes expression. Real-time PCR quantification of mitochondrial (A) citrate synthase, (B) succinate dehydrogenase and (C) cytochrome c oxidase expression in the stably-transfected mock, APP695 and APP751 expressing cell lines. The expression of the targeted gene was quantified relative to the endogenous β-actin level for each sample. Each value represents the mean ± SEM of three assays for each cell line sample. Significant differences (Student's *t*-test) were observed in citrate synthase, succinate dehydrogenase and cytochrome c oxidase gene expression between mock, APP695- and APP751-expressing cells ($^{*}p < 0.05$, $^{**}p < 0.005$, $^{***}p < 0.001$ using Student's *t*-test). Each value represents the mean ± SEM of three reactions for each cell line sample.

genes and the assays were performed according to the manufacturer's instructions.

The real-time RT-PCR reactions were performed using the TaqMan Universal PCR Master Mix (Applied Biosystems) in a 20 μl reaction volume containing 200 ng of cDNA. All reactions were performed in duplicate and included a negative control. PCR reactions were carried out using an ABI StepOnePlus™ Real Time PCR system (Life Technologies). Cycle conditions, according to ABI recommendations for Taqman Gene Expression Assay, were 2 min at 50 °C, 10 min at 95 °C and 40 cycles of 15 s at 95 °C and 1 min at 60 °C. Relative quantification of mRNA levels was determined by the system software, which uses the comparative C_T methods ($\Delta\Delta C_T$).

2.4. Cytochrome oxidase IV activity assay

The cytochrome oxidase IV (COX IV) activity was measured using the assay kit from Sigma–Aldrich (St. Louis, USA) using isolated mitochondrial fractions from the cultured cells. Mitochondria were isolated using the Isolation Kit for cultured cells from Thermo Fisher Scientific (Waltham, USA). The COX IV activity assay reactions were set up following the procedures provided by the manufacturer. The absorbance readings were taken at 10 s intervals for 6 consecutive reads at 550 nm after adding the reduced ferrocytochrome c substrate. A blank reaction without the mitochondrial isolates was included as controls. The COX IV activity was calculated using the equation provided in the protocol and expressed in terms of units per ml. All reactions were run in triplicates.

2.5. Measurement of mitochondrial membrane potential

The JC-1 dye (Life Technologies) was used for the measurement of mitochondrial membrane potential. Briefly, 2×10^4 cells were seeded overnight before incubating with JC-1 in Earle's balanced salt solution (EBSS) for 30 min at 37 °C. The cells were then washed twice in EBSS before fluorescence values were measured. Two separate reads were performed. One read was to measure green fluorescence at an excitation wavelength of 488 nm and an emission wavelength of 590 nm, and the other measured the red fluorescence at an excitation wavelength of 560 nm and an emission wavelength of 595 nm. The ratio of the red to green fluorescence was calculated to determine the mitochondrial membrane potential.

2.6. NAD^+/NADH quantification

Intracellular NAD^+/NADH ratio was quantified using the NAD/NADH assay kit (Biovision Inc, California, USA). Briefly, cellular lysates were incubated with the supplied assay buffer following the procedures provided by the manufacturer. Absorbance readings were taken at 450 nm. The NAD^+/NADH ratio was calculated as indicated in the protocol.

2.7. Statistical analysis

Significant differences were analyzed using Student's *t*-test. A *p* value of <0.05 is considered significant.

3. Results

3.1. Expression of human APP spliced variants in APP knockout cell line

Human APP is known to undergo alternative splicing resulting in several spliced variants [2,3]. They can be grouped as those that contain the Kunitz Protease Inhibitory (KPI) domain (KPI+) and those that do not (KPI−). The main APP variant in human brain is APP695 that does not contain the KPI domain (KPI−) [24]. However, in AD brain tissues, an up-regulation of longer APP spliced variants containing the KPI (KPI+) including APP751 has been reported [6–8].

To better understand the function of the APP spliced variants without the presence of the endogenous mouse APP, we have stably transfected human APP695 (KPI−) and APP751 (KPI+) in the APP knockout cell line [22]. Since the APP KPI+ isoforms are increased in AD, we decided to compare the effect of the APP with and without the KPI domain. A mock cell line was generated by stably transfected the APP knockout neuronal cells with the same expression vector without any APP insert.

Immunoblotting using the N-terminal anti-APP antibody (22C11) [25] and the C-terminal anti-APP antibody 6E10 [26] detects a major ~90 kDa protein band in cells expressing APP695, and a higher >95 kDa protein band in APP751 expressing cells (Fig. 1A).

Using a Taqman probe that targets all human APP spliced variants, we detected comparable level of APP mRNA in both APP695 and APP751 cell lines (Fig. 1B). To demonstrate the expression of the specific APP spliced variant in each of the cell line, we used Taqman probe targeting APP695 and APP751 mRNA. This specificity was shown in Figs. 1C and D. The Taqman probe against APP695 only detected APP expression in the APP695 cell line (Fig. 1C), whereas the Taqman probe targeting APP751 only bind APP in the APP751 cell line (Fig. 1D).

3.2. APP751 expression lowers the expression of major mitochondrial metabolic enzymes

Mitochondrial dysfunction is a prominent feature of AD brain [16–20]. This impairment has been linked to lower expression of major metabolic enzymes including those in the Tricarboxylic Acid (TCA) and oxidative phosphorylation [16,17,19] cycles. However, it is unclear if this reduction is linked to the up-regulation of the KPI-containing APP isoforms detected in AD [6–8].

We therefore examined the expression of several mitochondrial metabolic enzymes using real-time PCR. They are citrate synthase, succinate dehydrogenase and cytochrome c oxidase (COX IV). The first three enzymes are components of the Tricarboxylic Acid (TCA) cycle [17], and COX IV is a major component of oxidative phosphorylation [24].

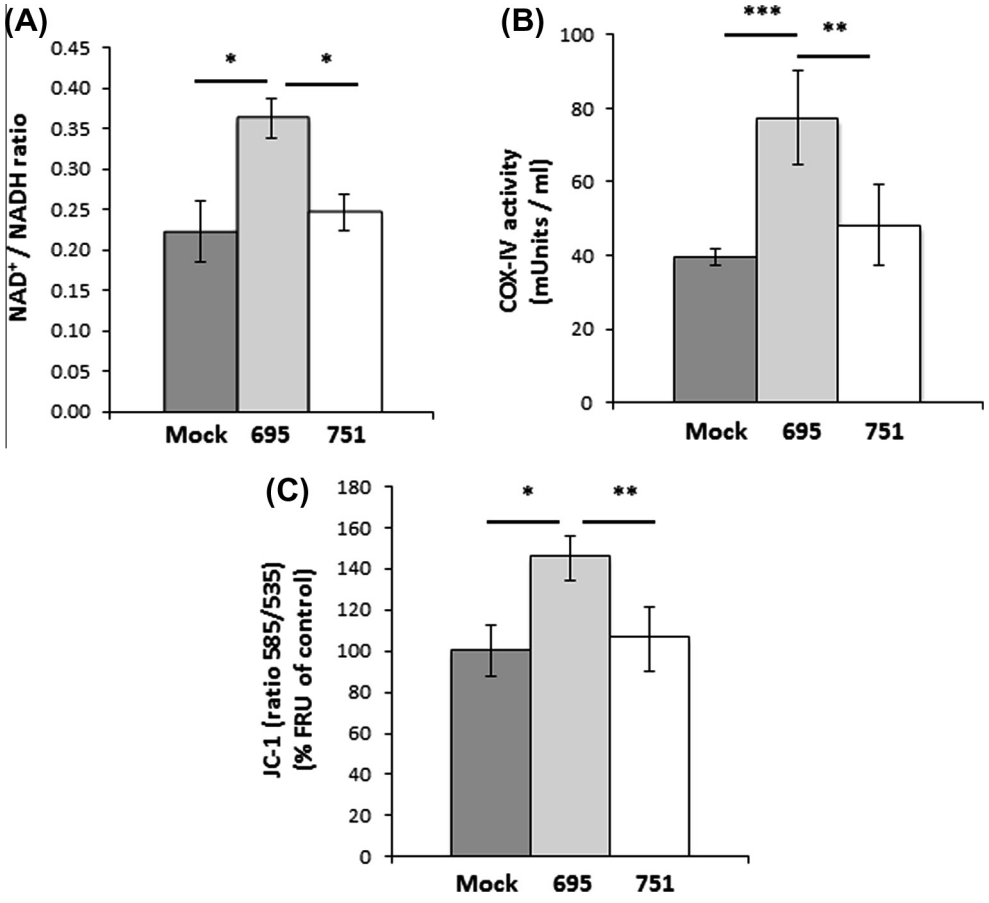

Fig. 3. Cells expressing APP751 impair mitochondrial function. (A) Higher intracellular NAD^+/NADH ratio with increased (B) cytochrome c oxidase (COX IV) activity and (C) mitochondrial membrane potential using the cationic JC-1 dye and were detected in APP695- as compared to APP751-expressing cell lines ($^*p < 0.01$, $^{**}p < 0.05$, $^{***}p < 0.005$ using Student's *t*-test). Each value represents the mean ± SEM of three assays for each cell line sample.

As shown in Fig. 2, cells transfected with APP695 has higher expression of citrate synthase (Fig. 2A), succinate dehydrogenase (Fig. 2B) and cytochrome c oxidase (Fig. 2C) as compared to cells transfected with the empty vector (mock). Citrate synthase was increased by 40%, succinate dehydrogenase by 67%, and cytochrome c oxidase by 64%.

However, citrate synthase and cytochrome c oxidase expression was not significant altered when comparing the APP751 and mock cell lines.

Interestingly, cells expressing the KPI-containing APP751 isoform lead to lower expression of citrate synthase (Fig. 2A), succinate dehydrogenase (Fig. 2B) and cytochrome c oxidase (Fig. 2C) by 29%, 40% and 63% respectively as compared to the cells transfected with the non-KPI APP695.

3.3. APP751 expression leads to lower mitochondrial function

As the metabolic enzymes examined in Fig. 2 plays an important role in the mitochondria, changes in their expression are likely to impact mitochondrial function.

To examine this, we first examined the NAD^+/NADH ratio, which are determined largely by the activity of the complex I in oxidative phosphorylation, converting NADH to NAD^+ via an oxidation reaction [27]. We found that cells expressing APP695 has ~38% higher NAD^+/NADH ratio as compared to mock cells (Fig. 3A). However, cells expressing APP751 has lower NAD^+/NADH ratio (~47%) as compared to the APP695 cells. No significant change in NAD^+/NADH ratio between mock cells and APP751 cells was detected.

Since electrons generated from oxidation of NADH are coupled to proton pumping across the oxidative phosphorylation reactions, we therefore decided to determine if lower COX IV expression affects the enzyme function. We found that mitochondrial fractions isolated from cells expressing APP695 have higher COX IV activity (~48%) as compared to mitochondrial fractions extracted from mock cells (Fig. 3B). But, the COX IV activity detected from the mitochondrial fractions of the APP751 cells is ~60% lower than mitochondrial fractions extracted from the APP695 cells. However, we did not detect any significant change in COX IV activity between the mitochondrial fractions isolated from mock cells and the APP751 cells.

Electrons transferred via oxidative phosphorylation are known to produce a membrane potential across the mitochondria that will affect mitochondrial function. To determine the mitochondrial membrane potential, $\Delta\psi_m$, we incubated the growing cells with the cationic fluorescent dye, JC-1. This particular dye is concentrated by mitochondria in proportion to their $\Delta\psi_m$.We found that cells expressing APP695 has higher fluorescence (~31%) as compared to mock cells (Fig. 3C). However, cells expressing APP751 was observed to lower the fluorescence by ~37% as compared to the APP695 cells. No significant change in JC-1 fluorescence was detected between mock cells and APP751 cells.

4. Discussion

Mitochondrial dysfunction is a prominent feature in Alzheimer's disease (AD) [14,15,20] and this aberration is linked to defective expression and function of metabolic enzymes [16–19]. However, the cause(s) leading to the down-regulation is unclear.

Longer APP isoforms containing the KPI-domain have been reported to increase in AD brain [5–8] but the functional consequence of this increase is unclear.

Studies have shown APP695 and APP751 have different susceptibility toward α- and β-secretase cleavage, affecting Aβ production [12,13]. However, the connection between the increasing generation of KPI-containing APP isoform and the mitochondrial dysfunction in AD is unknown.

In this study, we found that expression of citrate synthase, succinate dehydrogenase and cytochrome c oxidase are significantly reduced in cells expressing the KPI-containing APP751 as compared to the non-KPI APP695 expressing cells. These proteins are major metabolic enzymes within the mitochondrion, and the impairment will reduce the enzyme activity and impair mitochondrial function.

Several functions have been suggested for the KPI domain on APP [9–11], including the inhibition of some serine proteases. While the metabolic enzymes examined in this study are not known to be serine proteases, our observation suggests the KPI domain on APP can also inhibit these enzymes. However, the mechanism of this inhibition is unknown.

One possibility could involve interaction between APP and the metabolic enzymes in the mitochondrion. This is possible since APP can be targeted to the membrane of the mitochondrion [28,29]. But, it is unclear if APP isoforms with and without KPI has different rate of mitochondrial targeting. Nevertheless, this intracellular traffic could have facilitated the interaction between APP and the metabolic enzymes. Further, this interaction could be regulated by the presence (or absence) of the KPI domain on APP.

Alternatively, APP could regulate these metabolic enzymes by interacting with proteins involved in mitochondrial fission and fusion proteins [20,21,30]. This interaction is increasingly shown to affect mitochondrial biogenesis, possibly leading to dysfunction [31].

In summary, this study show for the first time that the KPI-containing APP751 expression significantly reduces the expression of major metabolic enzymes and this inhibitory action impair mitochondrial function. Based on this data, we suggest that up-regulation of the KPI-containing APP isoforms contributes to the impairment of metabolic enzymes and mitochondrial dysfunction in AD. Therefore, targeting the KPI–APP expression may represent a potential pharmacologic approach for the treatment of AD.

Author contributions

L.M.C. and M.L.L. performed the experiments. L.M.C., M. L.L. and B.S.W. analyzed the data. B.S.W. conceived and designed the experiments. L.M.C. and B.S.W. wrote the paper.

Acknowledgments

This work was supported by grants to B.S.W. from the National Medical Research Council (NMRC/1148/2008) and the Biomedical Research Council (BMRC/05/1/21/19/389). L.M.C. was supported by a graduate scholarship from Singapore Ministry of Education.

References

[1] G.G. Glenner, C.W. Wong, Alzheimer's disease: initial report of the purification and characterization of a novel cerebrovascular amyloid protein, Biochem. Biophys. Res. Commun. 120 (1984) 885–890.
[2] A. Weidemann, G. Konig, D. Bunke, P. Fischer, J.M. Salbaum, C.L. Masters, K. Beyreuther, Identification, biogenesis, and localization of precursors of Alzheimer's disease A4 amyloid protein, Cell 57 (1989) 115–126.
[3] T.E. Golde, S. Estus, M. Usiak, L.H. Younkin, S.G. Younkin, Expression of beta amyloid protein precursor mRNAs: recognition of a novel alternatively spliced form and quantitation in Alzheimer's disease using PCR, Neuron 4 (1990) 253–267.
[4] M.P. Mattson, Cellular actions of beta-amyloid precursor protein and its soluble and fibrillogenic derivatives, Physiol. Rev. 77 (1997) 1081–1132.
[5] S.A. Johnson, T. McNeill, B. Cordell, C.E. Finch, Relation of neuronal APP-751/APP-695 mRNA ratio and neuritic plaque density in Alzheimer's disease, Science 248 (1990) 854–857.

[6] P. Preece, D.J. Virley, M. Costandi, R. Coombes, S.J. Moss, A.W. Mudge, E. Jazin, N.J. Cairns, Amyloid precursor protein mRNA levels in Alzheimer's disease brain, Brain Res. Mol. Brain Res. 122 (2004) 1–9.
[7] R.D. Moir, T. Lynch, A.I. Bush, S. Whyte, A. Henry, S. Portbury, G. Multhaup, D.H. Small, R.E. Tanzi, K. Beyreuther, C.L. Masters, Relative increase in Alzheimer's disease of soluble forms of cerebral Abeta amyloid protein precursor containing the Kunitz protease inhibitory domain, J. Biol. Chem. 273 (1998) 5013–5019.
[8] R.E. Tanzi, A.I. McClatchey, E.D. Lamperti, L. Villa-Komaroff, J.F. Gusella, R.L. Neve, Protease inhibitor domain encoded by an amyloid protein precursor mRNA associated with Alzheimer's disease, Nature 331 (1988) 528–530.
[9] V.Y. Hook, C. Sei, S. Yasothornsrikul, T. Toneff, Y.H. Kang, S. Efthimiopoulos, N.K. Robakis, W. Van Nostrand, The Kunitz protease inhibitor form of the amyloid precursor protein (KPI/APP) inhibits the proneuropeptide processing enzyme prohormone thiol protease (PTP). colocalization of KPI/APP and PTP in secretory vesicles, J. Biol. Chem. 274 (1999) 3165–3172.
[10] F. Xu, M.L. Previti, M.T. Nieman, J. Davis, A.H. Schmaier, W.E. Van Nostrand, AbetaPP/APLP2 family of Kunitz serine proteinase inhibitors regulate cerebral thrombosis, J. Neurosci. 29 (2009) 5666–5670.
[11] M.A. Salameh, J.L. Robinson, D. Navaneetham, D. Sinha, B.J. Madden, P.N. Walsh, E.S. Radisky, The amyloid precursor protein/protease nexin 2 Kunitz inhibitor domain is a highly specific substrate of mesotrypsin, J. Biol. Chem. 285 (2010) 1939–1949.
[12] L. Ho, K. Fukuchi, S.G. Younkin, The alternatively spliced Kunitz protease inhibitor domain alters amyloid beta protein precursor processing and amyloid beta protein production in cultured cells, J. Biol. Chem. 271 (1996) 30929–30934.
[13] N.D. Belyaev, K.A. Kellett, C. Beckett, N.Z. Makova, T.J. Revett, N.N. Nalivaeva, N.M. Hooper, A.J. Turner, The transcriptionally active amyloid precursor protein (APP) intracellular domain is preferentially produced from the 695 isoform of APP in a {beta}-secretase-dependent pathway, J. Biol. Chem. 285 (2010) 41443–41454.
[14] M.P. Mattson, Pathways towards and away from Alzheimer's disease, Nature 430 (2004) 631–639.
[15] K. Itoh, K. Nakamura, M. Iijima, H. Sesaki, Mitochondrial dynamics in neurodegeneration, Trends Cell Biol. 23 (2013) 64–71.
[16] W.M. Brooks, P.J. Lynch, C.C. Ingle, A. Hatton, P.C. Emson, R.L. Faull, M.P. Starkey, Gene expression profiles of metabolic enzyme transcripts in Alzheimer's disease, Brain Res. 1127 (2007) 127–135.
[17] P. Bubber, V. Haroutunian, G. Fisch, J.P. Blass, G.E. Gibson, Mitochondrial abnormalities in Alzheimer brain: mechanistic implications, Ann. Neurol. 57 (2005) 695–703.
[18] M.J. Calkins, M. Manczak, P. Mao, U. Shirendeb, P.H. Reddy, Impaired mitochondrial biogenesis, defective axonal transport of mitochondria, abnormal mitochondrial dynamics and synaptic degeneration in a mouse model of Alzheimer's disease, Hum. Mol. Genet. 20 (2011) 4515–4529.
[19] W.S. Liang, E.M. Reiman, J. Valla, T. Dunckley, T.G. Beach, A. Grover, T.L. Niedzielko, L.E. Schneider, D. Mastroeni, R. Caselli, W. Kukull, J.C. Morris, C.M. Hulette, D. Schmechel, J. Rogers, D.A. Stephan, Alzheimer's disease is associated with reduced expression of energy metabolism genes in posterior cingulate neurons, Proc. Natl. Acad. Sci. USA 105 (2008) 4441–4446.
[20] B. Sheng, X. Wang, B. Su, H.G. Lee, G. Casadesus, G. Perry, X. Zhu, Impaired mitochondrial biogenesis contributes to mitochondrial dysfunction in Alzheimer's disease, J. Neurochem. 120 (2012) 419–429.
[21] X. Wang, B. Su, S.L. Siedlak, P.I. Moreira, H. Fujioka, Y. Wang, G. Casadesus, X. Zhu, Amyloid-beta overproduction causes abnormal mitochondrial dynamics via differential modulation of mitochondrial fission/fusion proteins, Proc. Natl. Acad. Sci. USA 105 (2008) 19318–19323.
[22] J. Tan, G. Mao, M.Z. Cui, S.C. Kang, B. Lamb, B.S. Wong, M.S. Sy, X. Xu, Effects of gamma-secretase cleavage-region mutations on APP processing and Abeta formation: interpretation with sequential cleavage and alpha-helical model, J. Neurochem. 107 (2008) 722–733.
[23] M. Mullan, F. Crawford, K. Axelman, H. Houlden, L. Lilius, B. Winblad, L. Lannfelt, A pathogenic mutation for probable Alzheimer's disease in the APP gene at the N-terminus of beta-amyloid, Nat. Genet. 1 (1992) 345–347.
[24] M.P. Mattson, S.L. Chan, W. Duan, Modification of brain aging and neurodegenerative disorders by genes, diet, and behavior, Physiol. Rev. 82 (2002) 637–672.
[25] C. Hilbich, U. Monning, C. Grund, C.L. Masters, K. Beyreuther, Amyloid-like properties of peptides flanking the epitope of amyloid precursor protein-specific monoclonal antibody 22C11, J. Biol. Chem. 268 (1993) 26571–26577.
[26] K. Hsiao, P. Chapman, S. Nilsen, C. Eckman, Y. Harigaya, S. Younkin, F. Yang, G. Cole, Correlative memory deficits, Abeta elevation, and amyloid plaques in transgenic mice, Science 274 (1996) 99–102.
[27] M.P. Mattson, Contributions of mitochondrial alterations, resulting from bad genes and a hostile environment, to the pathogenesis of Alzheimer's disease, Int. Rev. Neurobiol. 53 (2002) 387–409.
[28] H.K. Anandatheerthavarada, G. Biswas, M.A. Robin, N.G. Avadhani, Mitochondrial targeting and a novel transmembrane arrest of Alzheimer's amyloid precursor protein impairs mitochondrial function in neuronal cells, J. Cell Biol. 161 (2003) 41–54.
[29] L. Devi, B.M. Prabhu, D.F. Galati, N.G. Avadhani, H.K. Anandatheerthavarada, Accumulation of amyloid precursor protein in the mitochondrial import channels of human Alzheimer's disease brain is associated with mitochondrial dysfunction, J. Neurosci. 26 (2006) 9057–9068.
[30] X. Wang, B. Su, H.G. Lee, X. Li, G. Perry, M.A. Smith, X. Zhu, Impaired balance of mitochondrial fission and fusion in Alzheimer's disease, J. Neurosci. 29 (2009) 9090–9103.
[31] M. Liesa, M. Palacin, A. Zorzano, Mitochondrial dynamics in mammalian health and disease, Physiol. Rev. 89 (2009) 799–845.